ALTERATION, MINERALIZATION AND FLUID EVOLUTION OF VEGAS PELADAS IRON SKARNS, CORDILLERA PRINCIPAL SW MENDOZA ARGENTINA

Pons María Josefina[1], Franchini Marta[1], Meinert Lawrence[2]

[1]CONICET, Centro Patagónico de Estudios Metalogenéticos-CIMAR, Facultad de Ingeniería, Universidad Nacional del Comahue, Av. Buenos Aires 1400 (8300) Neuquén, Argentina. jpons@uncoma.edu.ar
[3] Department of Geology, Smith College, Northampton, MA 01063

INTRODUCTION

Vegas Peladas is one of 23 Fe, Fe-Cu and Cu (Ag) prospects in a 20 km by 200 km zone along the Andean Belt of southwest Mendoza province, Argentina (34–36°S and 69.5-70°W; Fig.1; Franchini et al., 2007) previously classified as metasomatic deposits. Recent studies have examined some of these prospects and identified skarn deposits (as described by Einaudi et al., 1981; Meinert et al., 2005), iron oxide-copper-gold-(IOCG) type systems (as described by Hitzman et al., 1992; Pollard, 2000), and manto-type Cu deposits (as described by Espinoza et al., 1996) (see Franchini et al., 2007). Vegas Peladas is similar to classic Fe skarns. This article describes the geology of the Vegas Peladas deposit and its alteration characteristics, to document the skarn end member of the various prospects in the Mendoza belt and to shed light on the genetic models for these various deposits.

LOCAL GEOLOGY

The Vegas Peladas iron prospect is hosted in the marine sedimentary rocks of the Puchenque (450 m) and Calabozo (50-100 m) Formations that out crop along both margins of the Vegas Peladas Creek. The Puchenque Formation (Fig. 2) consists of intercalations of calcareous claystone, silttone, shale and sandstone with calcareous cement and the Calabozo Formation is an homogeneous mudstone-wackestone. On the NE side of the creek, the gypsum of the Auquilco Formation unconformably overlies these units. The sedimentary units have been affected by Andean tectonism and have been intruded by the following igneous sequence: 1) diorite pluton, 2) granodiorite pluton, 3) granite pluton, and 4) andesite dikes and sills (Fig. 2). The presence of abundant diorite xenoliths within the granodiorite pluton and the textural evidence of plastic flow suggest that mingling with local chemical exchange occurred between the diorite and granodiorite magmas. Rb-Sr isochrons yielded an age of 15.19 ± 0.24 Ma for the granodiorite pluton with an initial $^{87}Sr/^{86}Sr$ ratio of 0.704351 ± 0.000044. The $^{47}Sm/^{144}Nd$ (0.123358) and $^{143}Nd/^{144}Nd$ (0.5127229) ratios are consistent with a mantle source for these calc-alkaline, metaluminous rocks with little crustal contamination. In the SE area of the valley, Quaternary basalts overlay in angular disconformity the sedimentary sequence and the intrusive units. Sediments of glacial, mass-wasting and fluvial origin partially cover the cirques, slopes, creeks and valleys (Fig. 2).

ALTERATION-MINERALIZATION AND FLUID EVOLUTION

Two metasomatic events were identified in the Vegas Peladas district. These are associated with two of the four igneous rock-types that intrude the Jurassic sedimentary rocks of the area. Metamorphism and metasomatism resulted in the transformation of sedimentary and igneous rocks into hornfels, marble and skarn. Each one of the mineralized skarns has distinctive characteristics, reflecting differences in hydrothermal fluid composition and source.

The most important hydrothermal alteration and mineralization in the area is an Fe skarn with a wide contact metamorphic aureole (hornfels-marble) that has replaced the Puchenque and Calabozo Formations at the contact with the diorite pluton (Fig. 2). The skarn consists of a prograde zoned exoskarn (Fig. 2), with an inner pyroxene + magnetite + quartz (Fig. 3) or garnet ($Ad_{31\text{-}89}Py_{0.34\text{-}2}Grs_{68\text{-}8.8}$) ± quartz (Fig. 3) zone and an intermediate garnet ($Ad_{38\text{-}51}Py_{1\text{-}2}Gr_{61\text{-}47}$) ± pyroxene massive zone and external garnet ($Ad_{96.2-100}Py_{0.0-0.08}Grs_{0.0-3.7}$) ± pyroxene ($Di_{24-70}Jo_{4.1-0.7}Hd_{72-29.3}$) veins (Fig. 3). The diorite margin has incipient and selective actinolite ± chlorite ± calcite ± orthoclase ± epidote alteration and a thin massive orthoclase + quartz envelope (Fig. 2). Based on the fluid inclusion (FI) data (Fig. 4A), these zones were formed at depths of ~ 3.3 km under lithostatic pressure of 880 bars, by brines (>50 wt % NaCl equiv with NaCl ± KCl ± $FeCl_n$ ± hematite) with high temperatures (670-400°C); these brines coexisted with vapor of low density. Under these pressures and temperatures, it is likely brines and vapours were formed by immiscibility of a low to moderate salinity magmatic fluids (6-8% wt NaCl equiv) that exsolved from the still crystallizing diorite pluton (Burnham, 1979; Bodnar *et al.*, 1985; Cline and Bodnar, 1991; Bordnar, 1995). The isotopic data ($\delta^{18}O$ 7.23/8.53‰) of the water in equilibrium with the inner garnet zone of the exoskarn suggests the presence of fluids of magmatic origin (Taylor, 1986; Meinert *et al.*, 2003). During this early stage, the continuous interaction with the wall rock reduced isobarically the temperature of the brines (up to ~250°C).

Superimposed on the prograde exoskarn zones the following retrograde assemblages (Fig. 2) were recognized: 1) epidote + magnetite ± quartz that replace the inner zone; 2) epidote ± quartz ± albite that replace the massive intermediate zone of garnet ± pyroxene and 3) actinolite ± quartz ± feldspar ± epidote that replace the prograde veins and cut hornfels in distal zones. In the diorite pluton, an epidote ± quartz ± amphibole ± pyrite endoskarn, a few centimetres wide, replaces early alteration together with widespread veins and veinlets of amphibole ± quartz ± magnetite ± epidote ± feldspar (Fig. 2).

The iron mineralization -magnetite, specular hematite and mushketovite- is mainly associated with retrograde mineral assemblages (Fig. 2). In the endoskarn, the magnetite is in contact and in equilibrium with epidote, quartz, alkali feldspar and amphibole (Fig. 3). In the inner zone of the exoskarn, it is in equilibrium with clinopyroxene ± quartz (Fig. 3). But the major iron outcrops (up to 32 x 4.5 m; Fig. 2) consist of magnetite in equilibrium with epidote ± quartz replacing the inner zone of the exoskarn (Fig. 3). This magnetite contains between 83 to 88% of FeO_{total}. Specular hematite is in equilibrium with epidote ± quartz ± albite (Ab_{90-98}), forming massive bodies (up to 4 x 1 m; Fig. 2) that replace the intermediate zones of the exoskarn (Fig. 3). Distal Fe mineralization fills veins several meters long and 5 to 40 cm thick with a core of mushketovite or specularite and actinolite ± quartz ± feldspar ± epidote selvages (Fig. 3). The mushketovite (that replace the specularite) has more iron (93.5 y 95% FeO_{total}) than earlier magnetite.

Recorded boiling fluids in FI hosted in retrograde quartz, indicate that iron oxides and retrograde minerals precipitated under hydrostatic pressures of 325 to 125 bars from saline (41.6-23 wt % NaCl equiv) fluids at temperatures between 420°C and 320°C. This change in the pressure regimen was induced by exsolution of volatiles from the magma, sealing of conducts by silicate mineral precipitation, and consequent fracturing of the exoskarn and boiling of the fluids. Under hydrostatic pressures, the increase of permeability allowed the infiltration of external fluids (formations water ± meteoric water?) to the hydrothermal system, their mixing with the magmatic fluids and cooling, promoting early silicate mineral instability and their replacement by hydrous minerals, quartz and the massive precipitation of most iron oxides, that also filled fractures, veins and cavities.

The $\delta^{18}O$ (~5 /13‰) values obtained for a fluid in equilibrium with magnetite of the exoskarn, suggest the influence of external fluids, like formation waters in equilibrium with the sedimentary sequence (Bowman, 1998). The trend toward lower $\delta^{18}O$ values in the fluid in equilibrium with retrograde epidote (-0.55/-3.7‰), quartz (-2.5/4.3‰), and actinolite (-0.55/3.7‰) than the previous assemblages, might be due to a temperature decrease after boiling and/or an influx of meteoric water into the system (Bowman, 1998).

The isotopic data of water in equilibrium with epidote of the endoskarn, indicates that epidote ± quartz ± amphibole ± pyrite and the veins of amphibole ± magnetite ± epidote ± quartz ± feldspar were formed under similar physical-chemical conditions to the retrograde mineral assemblages of the exoskarn. In this retrograde stage, the external zones collapsed downward and inside the hydrothermal system, in a reverse sequence that followed the prograde zones during their formation. Fluids that generated the retrograde paragenesis in the exoskarn, gradually invaded the heart of hydrothermal system.

Later albite ± epidote ± quartz ± calcite ± titanite ± chlorite ± pyrite veins cut all the prograde and retrograde assemblages, hornfels, and marble. FI data in calcite indicate fluids with lower temperatures (165-315°C) and salinities (8.4-13.5 wt. % NaCl equiv) than previous stages. The $\delta^{18}O$

values for the water in equilibrium with this epidote (-4.7/-0.2‰ and calcite (-3.9/-2.7‰), suggest mixing and dilution of previous fluids with meteoric water (with a dominance of the later) during cooling and collapse of the hydrothermal system (Bowman, 1998; Fournier, 1999; Meinert *et al.,* 2005).

Another Fe skarn formed in the contact of the sedimentary rocks with the granite pluton and associated rhyolite dikes. This skarn consist of: 1) a hornfels aureole a few meters wide, 2) an inner garnet ($Ad_{30-81}Py_{0.6-0}Gr_{69-19}$) ± pyroxene ($Di_{82-93}Jo_{3.7-1.7}Hd_{14-5.1}$) exoskarn zone with abundant scapolite (Me_{28-36}), 3) an intermediate scapolite ± clinopyroxene ($Di_{18.5-4.1}Jo_{8.8-2.2}Hd_{74-93.7}$) zone that cut the hornfels (Fig. 3), 4) a distal garnet ($And_{10.5-83.1}Py_{0.72-1.4}Grs_{89-15.49}$) ± pyroxene ($Di_{42.6-96}$ $Jo_{2.6-1.27}Hd_{54.8-2.73}$) zone (Fig. 3), 5) veins of scapolite (Me_{25-36}) ± ferroactinolite ± pyrite cut the previous alterations, 6) mushketovite and mushketovite ± calcite veins cut the inner zones of the skarn (Fig. 3), and 7) late retrograde epidote + calcite + titanite ± quartz ± chlorite ± pyrite. Microthermometric data of FI hosted in quartz (Fig. 4B) from the exoskarn, indicate that the intrusion of the granite increased the temperature of the adjacent wall rock (>550°C) and generated saline fluids and vapour by immiscibility that could have dissolved the iron rich-minerals from previous skarn (Hemley et al., 1992). These brines carried Fe in solution and, when cooled, precipitated it as iron oxides. This second metasomatic event is minor in magnitude.

DISCUSSION AND CONCLUSIONS

The mineralized skarns in the Vegas Peladas district are similar to other Fe skarn deposits worldwide (Einaudi et al., 1981; Meinert, 1984; Meinert et al., 2005) in the following features: (1) the presence of prograde exoskarns rich in andradite-grossularite garnet, diopside-hedenbergite pyroxene, and retrograde amphibole, epidote, quartz, chlorite and calcite; (2) magnetite, hematite and mushketovite are the main iron ore minerals and the most important orebodies are associated with retrograde mineral assemblages; (3) sulfides, mainly pyrite, are scarce and occur in late stages and distal zones; (4) skarns are zoned in space and time; (5) the distribution of alteration and mineralization during early, prograde stages was strongly influenced by the hosts composition (both igneous and sedimentary) whereas late, retrograde alteration was more strongly controlled by structure; and (6) sodic metasomatism (scapolite and albite) is intense in the skarn associated with the granite but less common in the skarn associated with diorite. In contrast, the presence of orthoclase as alteration product of the diorite is not common in Fe skarn descriptions (Einaudi et al., 1981; Meinert, 1984).

The alteration mineralogy of the skarns and the iron enrichment toward garnet crystal rims and at deposit scale, toward outer zones, suggest an increase in high oxygen fugacity and iron precipitation as temperature decreased. This is supported by the increase of hematite relative to magnetite from inner to outer zones. Both deposits have high salinity fluids capable of transporting large amounts of Fe in solution and in both skarns, most iron ore is associated with retrograde alteration, indicating that a temperature decrease was the main cause of iron precipitation.

Previous work assigned a Palaeogene age to the Fe skarns of southern Mendoza. New dating (Franchini et al., 2007) and the present study demonstrate that the iron skarns are associated with the least differentiated plutons, dikes and sills of the voluminous and ubiquitous magmatism of the Upper Miocene. These Neogene igneous rocks derived from primitive magmas originated in the mantle, with little or no crustal contamination; their emplacement was structurally controlled. Thus, these plutons at the intersection of the main lineaments, thrusts, and fold cores in poorly explored areas, can host iron mineralization in associated skarn. The abundance of primary amphibole and magnetite in these igneous rocks and in the skarn gives them a strong magnetic response which is important from a prospecting point of view. The distribution of alteration assemblages and distal vein and veinlets with Fe oxides and retrograde minerals can be used as an exploration guide in regions with poor exposure or without outcrops. The skarn mineralogy also can be used to distinguish these deposits from the IOGC-manto deposits that are also present in this segment of the Andes Cordillera.

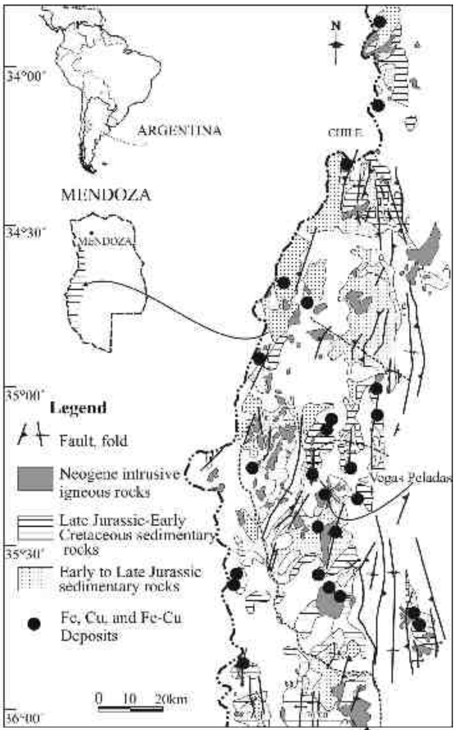

Figure 1. Geological map of SW Mendoza and location of the Vegas Peladas and other Fe, Cu and Fe-Cu deposits. Modify after Franchini et al., 2007

Figure 2. Map of the Vegas Peladas showing geology, alteration, mineralization and location of the samples shown in Fig. 3.

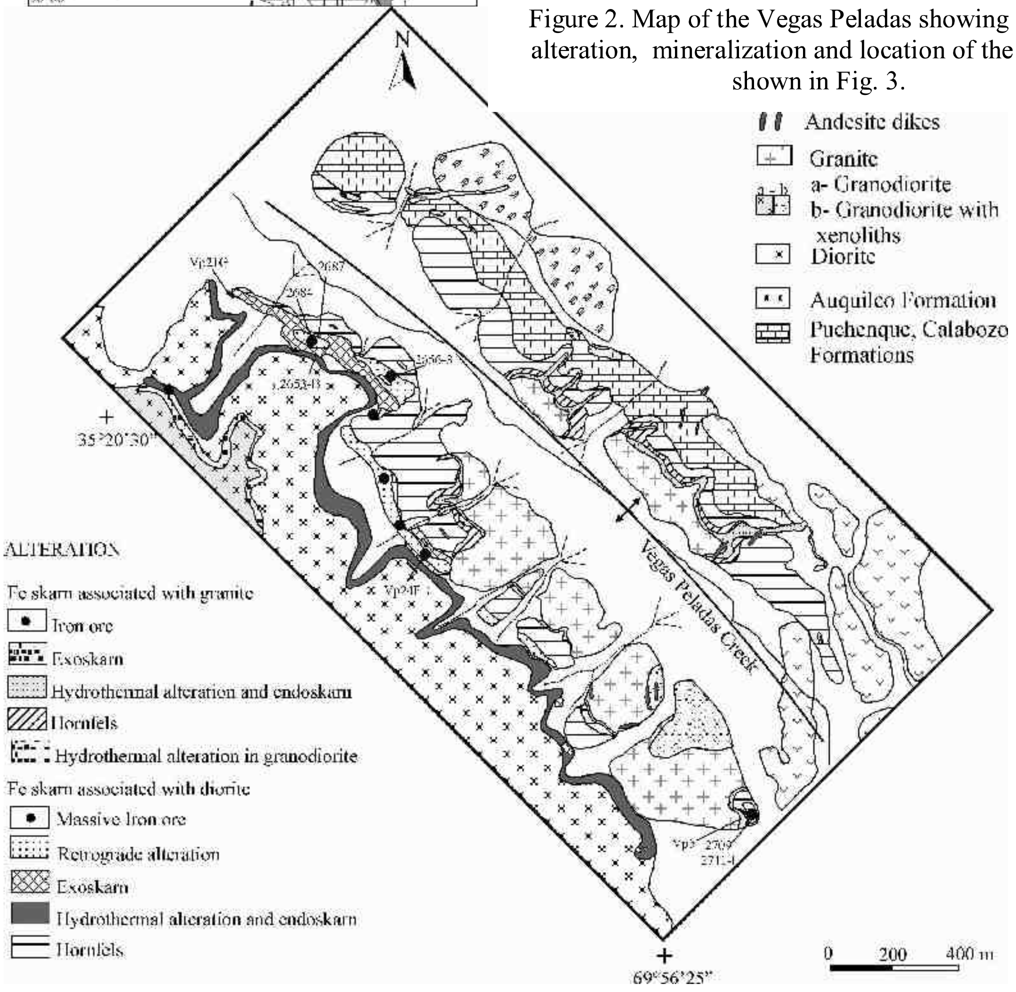

.

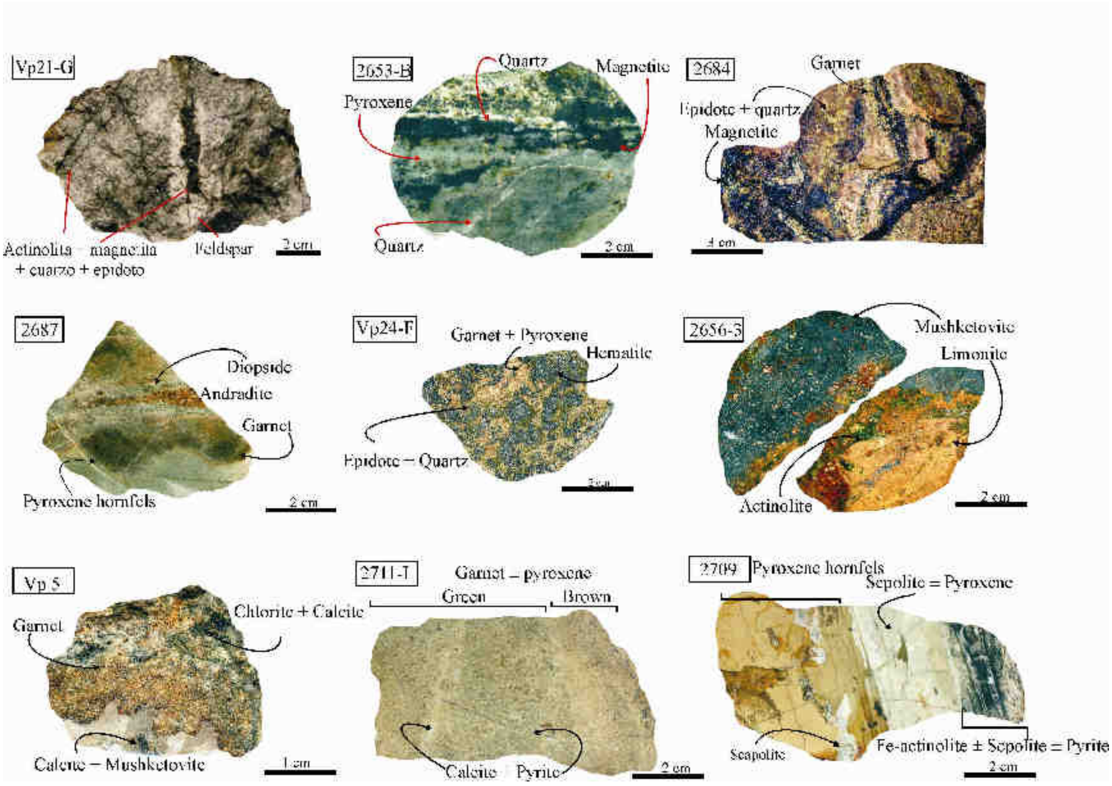

Figure 3. Photographs of different alteration styles from the skarn associated with diorite (samples: Vp21G, 2653-B, 2684, 2687, Vp24-F and 2656-3 and from the skarn associated with granite (samples: Vp5, 2711-I and 2709).

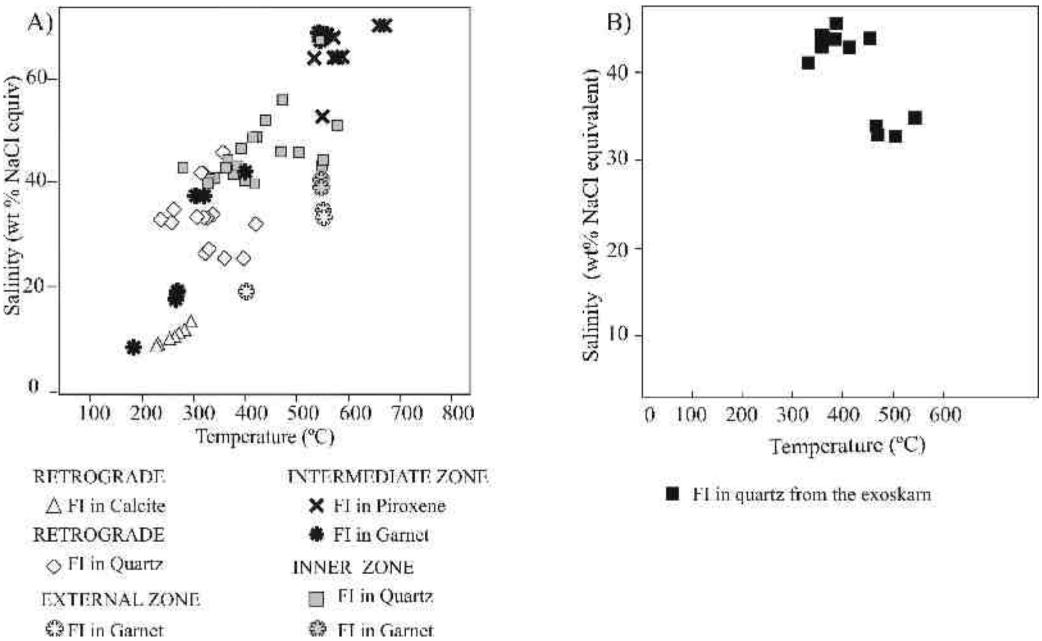

Figure 4. Salinity versus homogenization temperature diagram for Vegas Peladas prograde and retrograde alteration assemblages in Fe skarns associated with A) diorite and B) granite. FI= fluid inclusions.

REFERENCES

Bodnar, R. J., Burnham, C. W. and Sterner, S. M., 1985. Synthetic fluid inclusions in natural quartz: III. Determination of phase equilibrium properties in the system H2O-NaCl a 1000°C y 1500 bars. Geochimical Cosmochimical Acta 49, p. 1861-1873.

Bodnar, R. J., 1995. Fluid inclusion evidence for a magmatic source for metals in porphyry copper deposits: Mineralogical Association of Canada Short Course Series, v. 23, p. 139-152.

Burnham, C. W., 1979. Magmas and hydrothermal fluids. Geochemistry of Hydrothermal Ore Deposits. Eds. Barnes, H. L.. J Wiley and Sons, New York, p. 71-136.

Bowman, J. R., 1998. Stalble-Isotope systematics of Skarns. Mineralogical Association of Canada Short Course Series, Mineralized Intrusion-Related Skarn Systems, Ed. D.R. Lentz, Quebec, Canadá, v. 26: p.99-145.

Cline, J. S. and Bodnar, R. J., 1991. Can Economic Porphyry Copper Mineralization be Generated by a Typical Cal-Alkaline Melt? Journal of Geophysical Research, v. 96, N° B5, p. 8113-8126.

Einaudi, M., Meinert L. D. and Newberry, 1981, Skarns Deposits: Economic Geology. 75th Aniversary Volume, p. 317-391.

Espinoza, S., Véliz, H., Esquivel, J., Arias, J., and Moraga, A., 1996. The Cupriferous Province of the Coastal Range, Northern Chile. In Camus, F., Sillitoe, R., and Petersen, R., eds., Andean Copper Deposits: New Discoveries, Mineralization, Styles and Metallogeny: Society of Economic Geologists Special Publication Number 5, p. 19-32.

Fournier, R. O., 1999. Hydrothermal processes related to movement of fluid from plastic into brittle rock in the magmatic-hydrothermal environment. Economic Geology, v. 94. p. 1193-1211.

Franchini, M. B., de Barrio, R., Pons M. J., Schalamuk, I. B. A., Ríos, F. J and Meinert, L., 2007. Fe skarns and IOCG-, and Manto-type deposits in the Andes Cordillera of SW Mendoza (34-36°LS), Argentina. Exploration and Mining Geology Special volume of IOCG deposits, Editor: Jeremy Richards (UofA), v. 16, n° 3-4, p. 233-265.

Hemley, J.J., Cygan, G.L, Fein, J.B., Robinson, G.R. and D´Angelo, W.M., 1992. Hydrothermal Ore-Forming Processes in the Light of Studies in Rock-Buffered Systems: I. Iron-Copper-Zinc-lead Sulfide Solubility Relations: Economic Geology, v. 87, p. 1-22.

Hitzman M., Oreskes, N. and Einaudi, M., 1992. Geological characteristics and tectonic setting of Proterozoic iron oxide (Cu-U-Au-REE) deposits: Precambrian Research, v. 58, p. 241-287.

Meinert, L. D., 1984. Mineralogy and Petrology of Iron Skarn in Western British Columbia, Canada: Economic Geology v. 79, N° 5 p. 869-882.

Meinert, L. D., Hedenquist, J. W., Satoh, H. and Matsuhisa, Y., 2003. Formation of Anhydrous and Hydrous Skarn in Cu-Au Ore Deposits by Magmatic Fluids. : Economic Geology, v. 98, p. 147-156.

Meinert, L. D., Dipple G. and Nicolescu, S., 2005. World Skarn Deposits. Economic Geology 100th Aniversary Volume, p. 299-336.

Pollard, P., 2000. Evidence of a magmatic fluid and metal source for Fe-oxide Cu-Au mineralization. In Porter, T.M, ed, Hydrothermal iron oxide copper-gold and related deposits: A global perspective: Australian Mineral Foundation, Adelaide, p. 27-41.

Taylor, B.E., 1986. Magmatic volatiles: Isotopic variation of C, H, and S: Reviews in Mineralogy, v. 16: 185-226.